1-1-2005

# Thermodynamics and Proton Transport in Nafion - III. Proton Transport in Nafion/Sulfated ZrO(2) Nanocomposite Membranes

P. Choi

N. H. Jalani

Ravindra Datta
*Worcester Polytechnic Institute*, rdatta@wpi.edu

*Journal of The Electrochemical Society*, **152** (8) A1548-A1554 (2005)
0013-4651/2005/152(8)/A1548/7/$7.00 © The Electrochemical Society, Inc.

# Thermodynamics and Proton Transport in Nafion

## III. Proton Transport in Nafion/Sulfated $ZrO_2$ Nanocomposite Membranes

**Pyoungho Choi,* Nikhil H. Jalani,* and Ravindra Datta**,z**

*Fuel Cell Center, Department of Chemical Engineering, Worcester Polytechnic Institute, Worcester, Massachusetts 01609, USA*

A proton transport model is proposed to describe proton diffusion in Nafion/($ZrO_2/SO_4^{2-}$) nanocomposite membranes. The model considers the water content which could be determined by thermodynamics, dissociation of protons near the acid surface, stabilization of protons in water, and the strength and concentration of acid sites from Nafion as well as $ZrO_2/SO_4^{2-}$. The transport of proton occurs via a sluggish hopping process through the membrane surface, and relatively fast structural and ordinary mass diffusion of hydronium ions in the bulk of the membrane pores. The conductivity of the in situ sol-gel prepared Nafion/($ZrO_2/SO_4^{2-}$) nanocomposite membranes is accurately predicted as a function of relative humidity without any fitted parameters. Nafion/($ZrO_2/SO_4^{2-}$) nanocomposite membrane shows higher proton conductivity compared with Nafion at the same temperature and humidity conditions due to the improved water uptake and provision of strong acid sites. The model provides a theoretical framework for understanding proton conduction in nanocomposite membranes and can be successfully used to develop high-conducting membranes for fuel cell applications.
 [DOI: 10.1149/1.1945668] 

Manuscript submitted December 11, 2004; revised manuscript received March 1, 2005. Available electronically July 5, 2005.

Recently, extensive research efforts are being made worldwide to find new proton-conducting materials for proton-exchange membrane (PEM) fuel cell applications because the main obstacles to commercialization of PEM fuel cells are mostly related to the proton-conducting materials, typically solid polymer electrolytes such as perfluorosulfonic acid membranes.[1-3] They are expensive, mechanically unfavorable at high temperature, and conductive only when soaked in water, which limits fuel cell operating temperature to 100°C, which in turn results in low fuel cell performance due to low electrode kinetics and less CO tolerance. The operation of fuel cells at high temperature provides many advantages,[4,5] such as improved kinetics at the surface of the electrode, which is especially important in methanol and CO-containing reformate feeds, fast transport of protons across the PEM, efficient heat and water management, and also opening a new possibility of integrating fuel cells with methanol reformer, which can result in compact fuel cell systems. Thus, the development of stable membranes at high temperature is an active area of research in fuel cells.

The so-called "high-temperature membranes" can be developed via the modification of polymer (host membrane) with hygroscopic oxides such as $SiO_2$ and $TiO_2$ to increase water uptake, or inorganic solid acids such as $ZrO_2/SO_4^{2-}$ to increase the water uptake as well as the concentration of acid sites, or inorganic proton conductor such as heteropoly acids to further enhance proton conductivity using the inorganic-assisted proton transport together with the high water uptake and high acid concentrations in the membrane. Some examples of polymer/inorganic nanocomposite membranes are Nafion/$SiO_2$,[6,7] Nafion/$Al_2O_3$,[8] Nafion/$TiO_2$,[9] Nafion/$ZrO_2$,[10] Nafion/ZrP,[11] Nafion/PTA,[12] Nafion/HPA,[13] SPEK/$ZrO_2$,[14] SPEEK/ZrP,[15] SPEK/($ZrO_2$/PTA),[16] and PBI/(SiWA + $SiO_2$),[17] etc. These membranes can be prepared by casting a bulk mixture of powder or colloidal state of inorganics with a polymer solution, or in situ formation in a polymer membrane. The size and dispersion of solid particles are of special importance in both methods. The in situ method is based on sol-gel reactions in the membrane, and the formations of nanometer sized particles in the host membrane are claimed. These sol-gel prepared nanocomposite membranes are Nafion/$ZrO_2$,[18] Nafion/$SiO_2$,[19] and Nafion/$TiO_2$,[20] etc. The nanocomposite membranes show a much higher water uptake,[6] reduced methanol crossover,[14] improved mechanical and thermal stabilities at high temperature,[17] and improved fuel cell performance,[8,11,21] although the reason for the performance enhancement was not elucidated and the long-term stability of these membranes is still in question. In spite of their substantial increase in the amount of water uptake and better fuel cell performance at high temperature compared with an unmodified membrane, the improved proton conductivity of the nanocomposite membranes has not been yet proven and is a subject of current debate. For example, Miyake et al.[6] reported that conductivities of sol-gel prepared Nafion/$SiO_2$ nanocomposite membranes were 0.185, 0.16, and 0.112 S/cm for 4-5%, 10-12%, and 16-17% loadings of $SiO_2$, respectively, while that of Nafion was 0.21 S/cm at the same condition of 120°C and 78% relative humidity environments. Arico et al.[7] reported higher proton conductivity of inorganic acid doped-nanocomposite membranes such as Nafion/$SiO_2$, Nafion/(PWA + $SiO_2$), and Nafion/$ZrO_2$ over all the temperature ranges of experiment.

In the present work, we prepared Nafion/($SO_4^{2-}/ZrO_2$) membrane via in situ sol-gel technique and compared with unmodified Nafion in terms of water uptake and proton conductivity for different relative humidity conditions. The objective of this paper is to understand the proton-transport mechanism in nanocomposite membranes so that the favorable properties of inorganics for high proton conductivity can be derived to design new membranes for fuel cells. A theoretical proton conductivity model is developed based on the parallel pore model incorporating various proton-transport mechanisms such as surface proton hopping, Grotthuss diffusion, and traditional en masse diffusions.

## Experimental

*Membrane preparation.*— A Nafion/($ZrO_2/SO_4^{2-}$) nanocomposite membrane was prepared via in situ sol-gel synthesis developed by Uchida et al.[9] Nafion 112 serves as a template that directs the morphology and particle size of the oxide in the PEM matrix. As-received Nafion was purified by heating in pure water at 60-70°C for 30 min, treated in 3 wt % $H_2O_2$ solution at 60-70°C for 30 min, and washed with deionized water at 60-70°C for 30 min. It was then converted to $Na^+$ form by heating in 1 M NaOH solution at 60°C for 30 min and washed with deionized water. The $Na^+$ form of Nafion was soaked in $Zr[OCH(CH_3)_2]_4$ ZrP/2-propanol solution at 25°C for 24 h. The membrane was then removed, blotted, and placed in 2-propanol/$H_2O$ solution for 2 h at 80°C. After the hydrolysis and condensation reactions, the membrane was removed and vacuum dried thoroughly at 25°C for 24 h and then at 110°C for 2 h. The membrane was then boiled in 1 M $H_2SO_4$ solution at 60°C for 1 h to sulfate the $ZrO_2$ nanoparticles and rinsed in water.

* Electrochemical Society Student Member.
** Electrochemical Society Active Member.
z E-mail: rdatta@wpi.edu

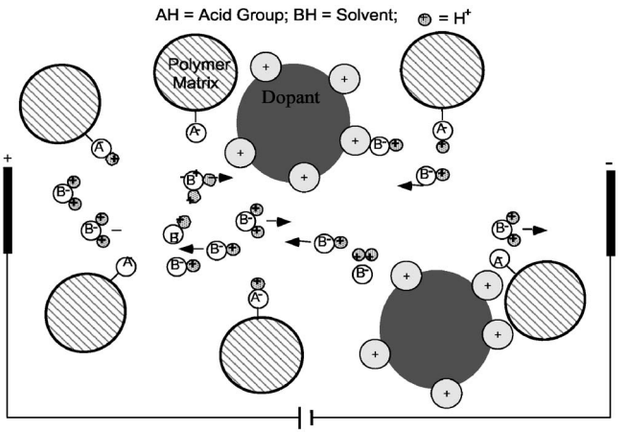


**Figure 1.** A schematic representation of Nafion/($ZrO_2/SO_4^{2-}$) nanocomposite membranes.

*Water uptake and proton conductivity measurements*.— The experimental details of water uptake and proton conductivity are provided previously.[22,23]

## Theory

Figure 1 shows a schematic representation of the nanocomposite membrane. The absorbed water molecules interact with the host membrane as well as the incorporated inorganics. The water molecules within the nanocomposite membrane can be classified as "bulk water" away from the acid groups and "surface water" near the acid groups. Thus, it is assumed that the protons in the nanocomposite membranes diffuse via (*i*) a surface diffusion mechanism close to the acid groups or under low water activity, and (*ii*) a bulk diffusion mechanism in the region away from the acid groups or under high water activity condition. In the bulk, proton diffusion is predominantly via the Grotthuss mechanism, but the $H_3O^+$ ion also undergoes traditional mass diffusion, i.e., the so-called en masse diffusion. The overall proton conductivity of nanocomposite membranes $\sigma_{H^+}$ can be written as[23]

$$\sigma_{H^+} = \frac{\varepsilon_i}{\tau}\left[\frac{F^2}{RT}(D^{\Sigma}_{H^+}C^{\Sigma}_{H^+} + D^{G}_{H^+}C_{H^+} + D^{E}_{H^+}C_{H^+})\right] \quad [1]$$

where $\varepsilon_i$ is porosity of membrane, $\tau$ is tortuosity factor, $F$ is Faraday's constant, $R$ is the gas constant, $T$ is temperature, $D^{\Sigma}_{H^+}$, $D^{G}_{H^+}$, and $D^{E}_{H^+}$ are the diffusion coefficients for the surface, Grotthuss, and en masse mechanisms, respectively, and $C_{H^+}$ and $C^{\Sigma}_{H^+}$ are the concentrations of protons participating in the bulk and surface phases, respectively.

## Parameter Identification

*Diffusion coefficients*.— The acid groups of nanocomposite membrane are composed of those of the host membrane (i.e., Nafion) and solid acid (i.e., $ZrO_2/SO_4^{2-}$). The surface diffusion coefficient of protons can be obtained from

$$\frac{1}{D^{\Sigma}_{H^+}} = \frac{x^{\Sigma}_{M}}{D^{\Sigma}_{H^+,M}} + \frac{x^{\Sigma}_{SA}}{D^{\Sigma}_{H^+,SA}} \quad [2]$$

where $D^{\Sigma}_{H^+,M}$ is the diffusion coefficient of proton via the acid group of the host membrane (M), $D^{\Sigma}_{H^+,SA}$ is the diffusion coefficient of proton via the acid group of the solid acid (SA), $x^{\Sigma}_{M}$ is the fraction of proton attached to the host membrane, and $x^{\Sigma}_{SA}$ is the fraction of proton attached to the acid groups of the solid acids. The fraction of membrane acid groups can be written in terms of the molar ratio of solid acid and membrane acid group, or $x^{\Sigma}_{M} = 1/(1 + q)$ and $x^{\Sigma}_{SA} = q/(1 + q)$, where $q$ = moles of acid sites from ($ZrO_2/SO_4^{2-}$)/mole of $SO_3^-$. For $w$ grams of solid acid with the average particle of diameter $d_p$, the moles of effective surface acid from the solid acids is $(6w/d_p\rho_p)C^{*}_{H^+,SA}$, where $\rho_p$ is particle density, and $C^{*}_{H^+,SA}$ [mol/m$^2$] is the effective surface site density of acid groups from the sulfated zirconia. Thus, the molar ratio of acid site for $w$ grams of solid acid per gram of host membrane can be written as

$$q = \frac{6w}{d_p\rho_p}EW_M C^{*}_{H^+,SA} \quad [3]$$

where $EW_M$ represents the equivalent weight of the host membrane.

The surface diffusion coefficients, $D^{\Sigma}_{H^+,M}$ and $D^{\Sigma}_{H^+,SA}$, can be obtained by applying the Einstein-Smoluchowski relation[24] $D = l^2_{\Sigma}/\kappa\tau^{\Sigma}_{D}$, where $l_{\Sigma}$ is the mean step distance, $\kappa$ is the dimensionality constant, and $\tau^{\Sigma}_{D}$ is the mean time between successive steps. The hopping time is provided by $\tau^{\Sigma}_{D} = \nu_0^{-1}\exp(\Delta G^{e,0}_{\Sigma}/k_BT)$, where $\nu_0$ is the thermal frequency, i.e., $\nu_0 = k_BT/h$ in which $k_B$ is the Boltzmann constant and $h$ is the Planck constant, and $\Delta G^{e,0}_{\Sigma}$ is the effective Gibbs free energy of activation for surface diffusion around the acid groups. Substitution of the acid fractions (i.e., $x^{\Sigma}_{M}$ and $x^{\Sigma}_{SA}$) and diffusion coefficients (i.e., $D^{\Sigma}_{H^+,M}$ and $D^{\Sigma}_{H^+,SA}$) into Eq. 2 gives

$$D^{\Sigma}_{H^+} = \frac{1}{4}\left[\frac{\left(\frac{k_BT}{h}\right)(d_p\rho_p + 6wEW_MC^{*}_{H^+,SA})}{\left(\frac{d_p\rho_p}{l^2_{\Sigma,M}}\right)\exp\left(\frac{\Delta G^{e,0}_{\Sigma,M}}{k_BT}\right) + \left(\frac{6wEW_MC^{*}_{H^+,SA}}{l^2_{\Sigma,SA}}\right)\exp\left(\frac{\Delta G^{e,0}_{\Sigma,SA}}{k_BT}\right)}\right] \quad [4]$$

where the number 4 in the denominator originates from the dimensionality constant for 2D surface diffusion, $\Delta G^{e,0}_{\Sigma,M}$ is the effective Gibbs free energy of activation for the surface diffusion around membrane acid groups, and $\Delta G^{e,0}_{\Sigma,SA}$ is the effective Gibbs free energy of activation for the surface diffusion around acid groups of the solid acid. The Gibbs free energy $\Delta G^{e,0}_{\Sigma}$ can be calculated by assuming that the first step is rate-determining for the overall surface proton hopping based on the quick decreases in coulombic interaction energy with the distance from the acid sites and low dielectric constant of water in the surface layer[25]

$$\Delta G^{e,0}_{\Sigma} \approx \frac{(q_{e^-})^2}{4\pi\varepsilon_0\varepsilon_r}\left[\frac{l_{\Sigma}}{(R_f + R_i + l_{\Sigma})(R_f + R_i)}\right] \quad [5]$$

where $\varepsilon_0$ is the permittivity of free space, $\varepsilon_r$ is the relative permittivity of the medium, $q_{e^-}$ is the electrostatic charge, $R_f$ is the effective radius of acid groups, and $R_i$ is the radius of the hydronium ion.

The diffusion coefficient for the Grotthuss mechanism depends on the rate at which the hydrogen bond forms and breaks between proton donating and receiving water molecules. The proton in aqueous solution is commonly visualized as hydronium ion $H_3O^+$ in which three hydrogen atoms share the charges equally, or Zundal ion $H_5O_2^+$ in which a proton is shared between two water molecules, or

Eigen ion $H_9O_4^+$ in which hydronium ion is strongly bound with three water molecules. In fact, there are many and complex states of hydrated protons $H^+(H_2O)_n$, and the three states are considered only as limit or ideal structures.[26-28] The rate-determining step for proton transport includes hydrogen-bond cleavage between the proton-accepting water molecule and a nearby water molecule, and reorientation of the proton-accepting molecule toward the hydronium ion to be in a receptive position. The rotational diffusion coefficient of the water molecule can be written as[29]

$$D_R = k_B T/8\pi\eta R_w^3 \quad [6]$$

where $\eta$ is the viscosity of water and $R_w$ is the radius of water molecule. Using the Einstein relation $\tau_D = 1/2D_R$, the relaxation time is given as

$$\tau_D = 4\pi\eta R_w^3/k_B T \quad [7]$$

It has been suggested that the microscopic water reorientation time is some fraction of the relaxation time (e.g., $2\tau_D/3$). The proton diffusion by the Grotthuss mechanism is characterized by the water reorientation time $\tau_D^G = 1.5$ ps at room temperature,[30] which is measured and also calculated from the relation between the force of water dipole with the hydronium ion and torque for translational rotation. Thus, the Grotthuss diffusion coefficient is calculated as $D_{H^+}^G \approx 7 \times 10^{-5}$ cm$^2$/s from $D_{H^+}^G = l_G^2/6\tau_D^G$, where $l_G = 0.255$ nm, O-O distance of $H_5O_2^+$ ion, and $\tau_D^G = 1.5$ ps.

The en masse diffusion coefficient of hydronium ion in the medium consisting of water, membrane acid site, and solid acids can be written as

$$\frac{1}{D_{H^+}^E} = \frac{x_W}{D_{H^+}^W}\left(1 + \frac{x_M}{x_W}\frac{D_{H^+}^W}{D_{H^+}^M} + \frac{x_{SA}}{x_W}\frac{D_{H^+}^W}{D_{H^+}^{SA}}\right) \quad [8]$$

where $x_W$, $x_M$, and $x_{SA}$ denote the fraction of water, membrane, and solid acid, respectively, and $D_{H^+}^W$, $D_{H^+}^M$, and $D_{H^+}^{SA}$ denote the Stefan-Maxwell diffusion coefficients of hydronium ion and bulk water, hydronium ion and polymer matrix, and hydronium ion and solid acids, respectively. It is assumed that the effective surface molecules of solid acid serve as molecular particles for the en masse diffusion. The fraction of water in the membrane can be written as $x_W = \lambda_W/(\lambda_W + 1)$, where the solvent loading $\lambda_W$ is given by

$$\lambda_W = \frac{p(1+w)}{MW_W\left(\frac{1}{EW} + \left(\frac{6w}{d_p\rho_p}\right)C_{H^+,SA}^*\right)} \quad [9]$$

where $p$ is the mass of absorbed solvent per mass of dry nanocomposite membrane and $MW_W$ is the molecular weight of water. Using the analogy between the Einstein-Smoluchowski relation and elementary kinetic theory, the diffusion coefficient ratios can be calculated as[23] $D_{H^+}^W/D_{H^+}^M \approx \sqrt{2(r_{M/W})^{2/3}}$ and $D_{H^+}^W/D_{H^+}^{SA} \approx \sqrt{2(r_{SA/W})^{2/3}}$, where $r_{M/W}$, and $r_{SA/W}$ are the ratios of partial molar volume of membrane to that of water, and partial molar volume of solid acid to that of water, respectively. Applying these into Eq. 8 and from $x_M/x_W = 1/\lambda_W(1+q)$ and $x_{SA}/x_W = q/\lambda_W(1+q)$, the en masse diffusion coefficient of hydronium ion for the medium composed of water, polymer matrix, and solid acids can be written as

$$D_{H^+}^E = \left\{\frac{(\lambda_W+1)\left(1 + \frac{6w}{d_p\rho_p}EW_M C_{H^+,SA}^*\right)}{\lambda_W\left(1 + \frac{6w}{d_p\rho_p}EW_M C_{H^+,SA}^*\right) + \sqrt{2}(r_{M/W})^{2/3} + \sqrt{2}(r_{SA/W})^{2/3}\frac{6w}{d_p\rho_p}EW_M C_{H^+,SA}^*}\right\} D_{H^+}^W \quad [10]$$

Thus, the en masse diffusion coefficient depends on the amount of water uptake ($\lambda_W$), particle size of inorganics ($d_p$), the amount of loading of inorganics ($w$), the ratio of partial molar volume of host membrane to water ($r_{M/W}$), the ratio of partial molar volume of inorganics to water ($r_{S/W}$), surface acid site density of the inorganics $C_{H^+,SA}^*$, and the hydronium ion diffusion coefficient in aqueous water ($D_{H^+}^W$).

The diffusion coefficient of hydronium ion through water $D_{H^+}^W$ is obtained from the Stokes-Einstein relation or usually approximated[29] as the self-diffusion coefficient of water, which has been reported as 2.1-2.3 $\times 10^{-5}$ cm$^2$/s at room temperature. Considering hydronium ion as a diffusing entity in the medium of water, the Stokes-Einstein relation[24,31] provides

$$D_{H^+}^W = \frac{k_B T}{6\pi\eta R_{H_2O}^*} \quad [11]$$

where $\eta$ is the viscosity of the medium and $R_{H_2O}^*$ is the hydrodynamic radius of hydronium ion. Because the Stokes-Einstein equation provides an approximation of the diffusion coefficient for molecular species and the concept of hydrodynamic radius is rather unclear, we take $D_{H^+}^W$ as the self-diffusion coefficient of water. In fact, this corresponds the effective water radius $R_{H_2O}^* = 0.108$ nm, smaller than the geometric radius of water molecule $R_{H_2O} = 0.143$ -0.144. Because the experimental diffusion coefficient of proton in water is known as $9.31 \times 10^{-5}$ cm$^2$/s at room temperature,[24] the Grotthuss diffusion coefficient can also be obtained by subtracting the self-diffusion coefficient of water molecule from the experimental proton diffusion coefficient.

*Distribution of protons between the surface and bulk regions*.—Some of the dissociated protons remain close to the anion surface sites and participate in surface diffusion, whereas others with a higher degree of hydration break away into the pore bulk and participate in bulk diffusion comprised of Grotthuss and en masse mechanisms. Here we assume that dissociated acid sites with up to two water molecules remain close to the surface and designate these sites as surface water, while those with more than two water molecules move away from the surface to the pore bulk. The total concentration of acid sites is calculated[32] from $C_{H^+,0} = 1/\lambda_W \bar{V}_w$, where $\bar{V}_w$ is partial molar volume of water, and the concentration of surface protons $C_{H^+}^\Sigma \approx C_{H^+,0}(\theta_1 + \theta_2)$, where $\theta_i$ denotes the fraction of acid sites with $i$ bound water molecules.[23] Because the acid sites are in the host membrane and solid acids, the total surface concentration is $C_{H^+}^\Sigma = C_{H^+,M}^\Sigma + C_{H^+,SA}^\Sigma$. In terms of surface fraction of total concentration, the surface concentration can be written as $C_{H^+,M}^\Sigma = f_M^\Sigma C_{H^+,0}$ and $C_{H^+,SA}^\Sigma = f_{SA}^\Sigma C_{H^+,0}$, where $f_M^\Sigma$ and $f_{SA}^\Sigma$ represent the surface fraction of protons near the host membrane and solid acid, respectively[23]

$$f_M^{\Sigma} = \frac{d_p\rho_p}{(d_p\rho_p + 6wEW_M C^*_{H^+,SA})}\left[\frac{K_{1,M}a_w(1-a_w)(1+K_{2,M}a_w)}{(1-a_w)(1+K_{1,M}a_w)+K_{1,M}K_{2,M}a_w^2(1-a_w^{v-1})}\right] \quad [12]$$

while the surface fraction of proton near solid acid is

$$f_{SA}^{\Sigma} = \frac{6wEW_M C^*_{H^+,0}}{(d_p\rho_p + 6wEW_M C^*_{H^+,SA})}\left[\frac{K_{1,SA}(1-a_w)(1+K_{2,SA}a_w)}{(1-a_w)(1+K_{1,SA}a_w)+K_{1,SA}K_{2,SA}a_w^2(1-a_w^{v-1})}\right] \quad [13]$$

where $v$ is the number of equilibrium steps with acid groups, $K_i$ is equilibrium constant between water and acid groups, and $a_w$ is the activity of water in surroundings. The bulk concentration of proton is given by $C_{H^+} = C_{H^+,0}(1 - \theta_0 - \theta_1 - \theta_2)$ and can be approximated as $C_{H^+} \approx C_{H^+,0} - C^{\Sigma}_{H^+,M} - C^{\Sigma}_{H^+,SA}$. Because the dissociation constants in water $K_1$ and $K_2$ may be different for sulfonic acid and solid acids, the concentrations of surface proton also vary with the strength of ions. The equilibrium constants $K_{1,M}$ and $K_{2,M}$ are taken as 1000 and 200, respectively, based on the dissociation constant of sulfonic acid and the proton affinity data.[33-35] The sulfated zirconia is usually regarded as[36] "superacid" ($H_0 < -16$) due to its strong acidity, which is greater than that of 100% sulfuric acid in which $H_0 \approx -12$, where $H_0$ is the Hammett indicator, although some studies[37,38] have indicated that the sulfated zirconia is not highly acidic and the catalytic activity is more related to its ability to stabilize transition state complex of reactants on the surface rather than its acidity. The fraction of surface proton is high at low water content and then decreases as the water content increases, while the bulk concentration increases monotonically with water content.

*Porosity and tortuosity*.— The total volume of the nanocomposite membrane is the sum of the three components, water, host membrane, and solid acid. The porosity of the membrane can be obtained from[23]

$$\varepsilon_i = \frac{\lambda_W(1/EW_M + w/MW_{SA})}{\lambda_W(1/EW_M + w/MW_{SA}) + r_{M/W}/EW_M + wr_{SA/W}/MW_{SA}} \quad [14]$$

The tortuosity factor $\tau$ is usually determined experimentally. Here, we use Preger's model[39] in which the tortuosity factor $\tau$ depends on the porosity $\varepsilon_i$, which in turn varies with the amount of water uptake, equivalent weight of host membrane, the amount of inorganics, molecular weight of inorganics, and the ratios of partial molar volumes as shown in Eq. 14.

## Results and Discussion

Table I shows the water sorption data of Nafion and Nafion/($ZrO_2/SO_4^{2-}$) nanocomposite membranes at 25 and 90°C. The incorporation of $ZrO_2/SO_4^{2-}$ increases water uptake as well as provides new acid sites for proton transport. The structure of $ZrO_2/SO_4^{2-}$ has been studied extensively and many surface models have been proposed.[40-42] Figure 2 shows the interconversion of Lewis acid site into Bronsted acid sites by the presence of water molecules, which was observed by IR spectra of pyridine adsorption.[43] The total acid site of the nanocomposite membrane is the sum of two acid sites, $C^*_{H^+,SA} = C^*_{H^+,SA(B)} + C^*_{H^+,SA(L)}$, where $C^*_{H^+,SA}$, $C^*_{H^+,SA(B)}$, and $C^*_{H^+,SA(L)}$ denote the concentration of the total, Bronsted, and Lewis acid sites, respectively. The surface site density is reported[44] in a range of $C^*_{H^+,SA(B)} \approx 10^{17}$ to $10^{18}$ molecules/m$^2$, and $C^*_{H^+,SA(L)} \approx 10^{17}$ to $10^{18}$ molecules/m$^2$, and thus $C^*_{H^+,SA} \approx 10^{18}$ molecules/m$^2$ is taken, which corresponds to $1.67 \times 10^{-6}$ mol/m$^2$. It is assumed that both sites are responsible for the generation of hydronium ions and participate in the transport of protons in the nanocomposite membrane. Table II shows all the parameters for estimating diffusion coefficients in the nanocomposite membranes. The amount of $ZrO_2/SO_4^{2-}$ added to the host membrane was determined as 3 wt % by ash analysis. Figure 3 shows the surface diffusion coefficient of nanocomposite membrane as a function of acid site density. As the acid site density increases, the surface diffusion coefficient increases with the density of acid sites provided by $ZrO_2/SO_4^{2-}$. The acid site density is directly related to the size of particle by Eq. 3; that is, the increase in site density $C^*_{H^+,SA}$ has the same effect in the decrease in the particle size $d_p$. Therefore, the small size with high surface acid density is favorable for high surface diffusion of protons in the nanocomposite membrane. The surface diffusion coefficient of Nafion is $1.01 \times 10^{-7}$ cm$^2$/s at 25°C, which is obtained by substituting $w = 0$ in Eq. 4. Figure 4 shows the en masse diffusion coefficients of nanocomposite membrane at 25 and 90°C. The diffusion coefficient increases with the vapor phase activity due to the increase of water content as shown in Eq. 10. The model predicts the diffusion coefficients of 1.35 and $4.71 \times 10^{-5}$ cm$^2$/s at 25 and 90°C, respectively, for the nanocomposite membrane contacting with saturated water vapor. This is about two orders of magnitude higher than the surface diffusion coefficients at the same temperature and activity conditions. In general, the surface diffusion process is considerably slower than the bulk process because of the strong coulombic interaction around the surface acid sites.[45,46] The coulombic barrier plays a central role in the surface diffusion and causes high activation energy for the transport of protons, while the bulk diffusion pro-

**Table I. Data for water sorption in Nafion and Nafion/($ZrO_2/SO_4^{2-}$) composite membranes.**

| Activity | Nafion (g water/g dry Nafion) | | Nafion/($ZrO_2/SO_4^{2-}$) (g water/g dry composite) | |
|---|---|---|---|---|
| | 25°C | 90°C | 25°C | 90°C |
| 0.1 | 0.0339 | 0.0344 | 0.0351 | 0.0413 |
| 0.2 | 0.0491 | 0.0488 | 0.0498 | 0.0586 |
| 0.3 | 0.0573 | 0.0499 | 0.0510 | 0.0599 |
| 0.4 | 0.0655 | 0.0614 | 0.0626 | 0.0737 |
| 0.5 | 0.0659 | 0.0749 | 0.0764 | 0.0899 |
| 0.6 | 0.0810 | 0.0875 | 0.0893 | 0.1051 |
| 0.7 | 0.0949 | 0.1127 | 0.1150 | 0.1352 |
| 0.8 | 0.1080 | 0.1309 | 0.1343 | 0.1584 |
| 0.9 | 0.1490 | 0.1710 | 0.1743 | 0.2053 |
| 1.0 | 0.2291 | 0.2701 | 0.2754 | 0.3247 |

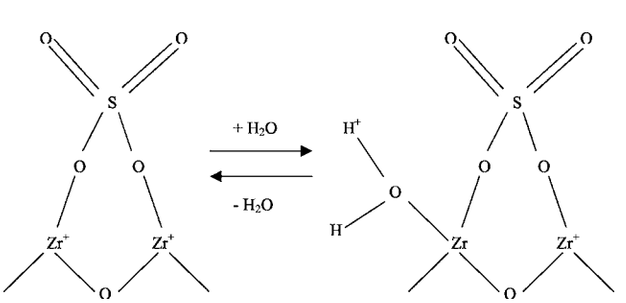


**Figure 2.** Structure of $ZrO_2/SO_4^{2-}$ solid acid.

**Table II. Parameter values employed in the model at room temperature.**

| Diff. coeff. | Symbols | Values | Units | Comments |
|---|---|---|---|---|
| $D^{\Sigma}_{H^+}$ | $EW_M$ | 1100 | g/equiv | Equivalent weight of membrane |
| | $MW_{SA}$ | 219.29 | g/mol | Molecular weight of solid acid |
| | $w$ | 0.03 | dimensionless | Weight ratio of solid acid to membrane |
| | $d_p$ | 2 | nm | The size of solid acid in the membrane |
| | $\rho_p$ | 5.83 | g/cm$^3$ | Density of zirconium oxide used |
| | $k_B$ | $1.38 \times 10^{-23}$ | J/K | Boltzmann constant |
| | $h$ | $6.626 \times 10^{-34}$ | J s | Planck constant |
| | $l_\Sigma$ | 0.255 | nm | Jump length of surface proton |
| | $R_{f(M)}$ | 0.254 | nm | Radius of acid site of membrane |
| | $R_{f(SA)}$ | 0.260 | nm | Radius of acid site of solid acid |
| | $R_{H_2O}$ | 0.143 | nm | Radius of water molecule |
| | $\varepsilon_0$ | $8.854 \times 10^{-12}$ | C$^2$/J m | Permittivity |
| | $\varepsilon_{r(M)}$ | 6 | Dimensionless | Relative permittivity of membrane |
| | $\varepsilon_{r(SA)}$ | 6 | Dimensionless | Relative permittivity of solid acid |
| | $q_{e^-}$ | $1.602 \times 10^{-19}$ | C | Electronic charge |
| $D^{G}_{H^+}$ | $l_G$ | 0.255 | nm | Proton jump length in Grotthuss mechanism |
| | $\tau^G_D$ | 1.5 | ps | Proton jump time in Grotthuss mechanism |
| $D^{E}_{H^+}$ | $\lambda_W$ | Eq. 9 | Dimensionless | mol $H_2O$/mol composite membrane |
| | $r_{M/W}$ | 29.83 | Dimensionless | Partial molar volume ratio of membrane to water |
| | $r_{SA/W}$ | 2.06 | Dimensionless | Partial molar volume ratio of solid acid to water |

cesses are of relatively low energy barriers. Figure 5 shows the experimental conductivity data of Nafion along with the model at 25 and 90°C, respectively. The Grotthuss diffusion coefficient can be calculated[47-49] by subtracting the en masse diffusion coefficient which is approximated by the self-diffusion coefficient of water molecule for the temperature range 0-100°C[50] from the total diffusion coefficient, which is obtained from the limiting ionic molar conductivity data given by[51] $\lambda^0_{H^+,T} = \lambda^0_{H^+,25C}\ [1 + 0.0139(T - 25°C)]$, where $\lambda^0_{H^+,25C}$ and $\lambda^0_{H^+,T}$ are the limiting molar conductivity of proton at 25°C and temperature $T$(°C). It is noteworthy that the use of concentration-independent diffusion coefficients in Eq. 1 is valid only for strong acid and low molar concentrations where the concentration-dependent coefficient $\chi$ is negligible in Kohlrausch's law $\lambda_+ = \lambda_{+,0} - \chi\sqrt{C_+}$, where $\lambda_+$ is molar conductivity, $\lambda_{+,0}$ is limiting molar conductivity, and $C_+$ is molar concentration of an ion.[24,52] The model predicts proton conductivity of Nafion to be 0.04 and 0.08 S/cm at 25 and 90°C for 80% relative humidity conditions, respectively. Figure 6 shows the proton conductivity of Nafion/($ZrO_2/SO_4^{2-}$) nanocomposite membranes. The proton conductivity of nanocomposite membrane is higher than that of Nafion over the whole activity range of water vapor. For example, at 80% relative humidity, the conductivities of 0.06 and 0.105 S/cm are predicted at 25 and 90°C, respectively. This is due to the increased water uptake along with the provisions of strong acid sites by $ZrO_2/SO_4^{2-}$. Figure 7 shows the effect of temperature on the proton conductivity at 80% relative humidity condition. Nafion/($ZrO_2/SO_4^{2-}$) nanocomposite membranes show higher proton conductivity than unmodified Nafion for all the range of temperature. The proton conductivity of Nafion can be improved by 20% with the incorporation of $ZrO_2/SO_4^{2-}$ in the host membrane if the model parameters such as particle size and particle distributions are carefully controlled during the preparation procedure. The analytical model suggests that the polymer/inorganic nanocomposite membranes can provide better proton conductivity than unmodified membranes. Further, the nanocomposite membranes are expected to enhance thermal and mechanical stability of the polymer membrane at high temperature.[53]

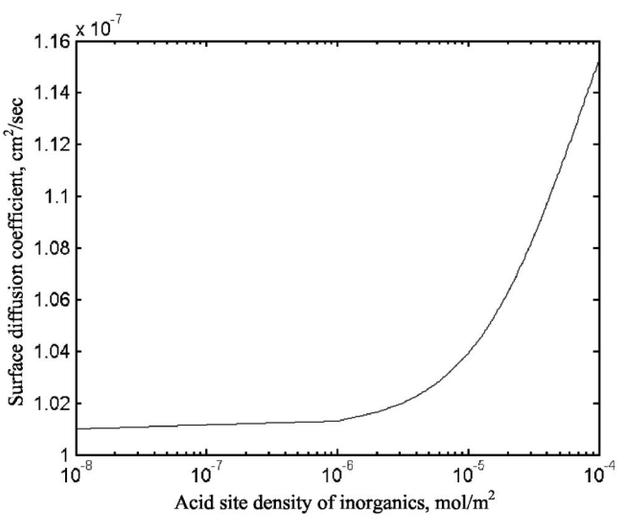


**Figure 3.** The effect of acid site density on the surface diffusion coefficient.

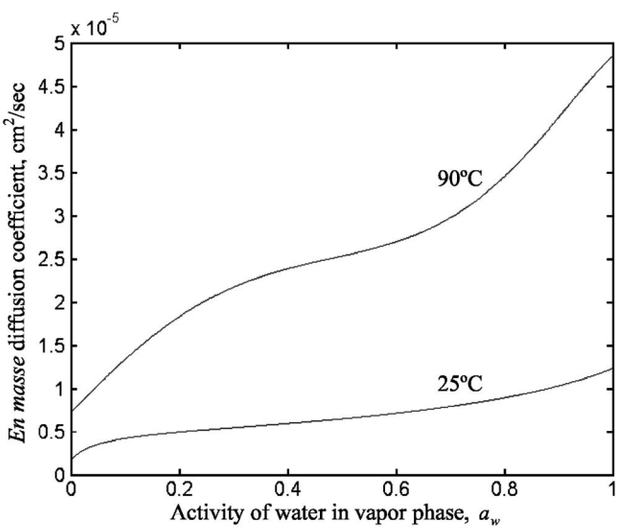


**Figure 4.** The effect of water vapor activity on the en masse diffusion coefficient.

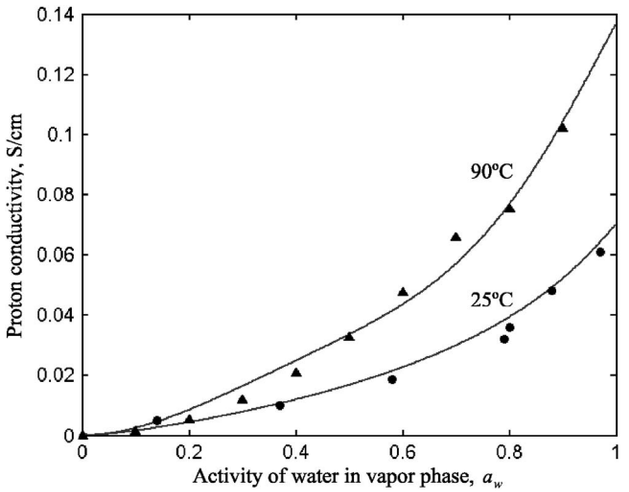


**Figure 5.** Proton conductivity of Nafion at 25 and 90°C.

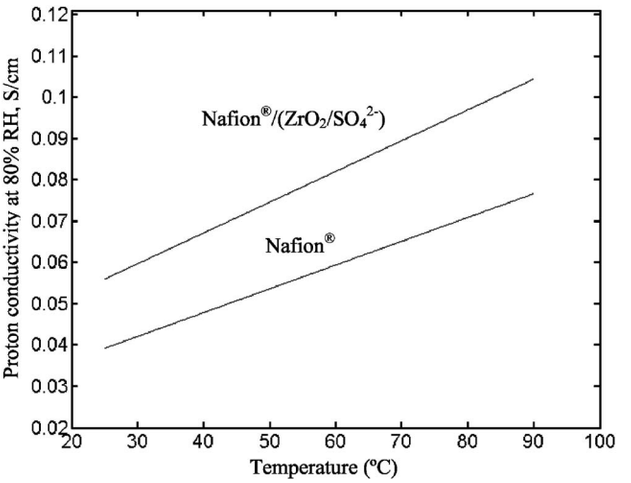


**Figure 7.** The effect of temperature on the proton conductivity of Nafion and Nafion/($ZrO_2/SO_4^{2-}$) composite membranes.

## Conclusions

A comprehensive proton transport model in Nafion/($ZrO_2/SO_4^{2-}$) nanocomposite membrane has been proposed based on the understanding of structural and physicochemical properties of the membranes. The solvent (i.e., water) sorption, the dissociation of protons around the acid sites, and the distribution of protons in the hydrated Nafion/($ZrO_2/SO_4^{2-}$) nanocomposites have been taken into consideration prior to the diffusion process. The transport model distinguishes the surface and bulk mechanisms of proton transport in the nanocomposite membrane in which the proton conduction depends on the water content, diffusion coefficients at the surface and bulk regions in the membrane, and concentration and distribution of protons. The surface diffusion of proton, which takes place dominantly under low-humidity environments, is slow due to high coulombic interaction around the acid surface, while the transport of protons in the bulk water is relatively fast and occurs via Grotthuss and en masse mechanisms. The sol-gel incorporation of $ZrO_2/SO_4^{2-}$ into Nafion increased the amount of water uptake and provided additional acid sites for proton diffusion, which resulted in higher proton conductivity compared to the host membrane. The results are encouraging and the polymer/inorganic membranes can be classified as a promising family of PEMs for fuel cells. The transport model developed here offers a theoretical framework for understanding the proton transfer in nanocomposite membranes and should also be helpful in systematically developing high proton-conducting nanocomposite membranes based on the incorporation of inorganic materials into the host membranes.

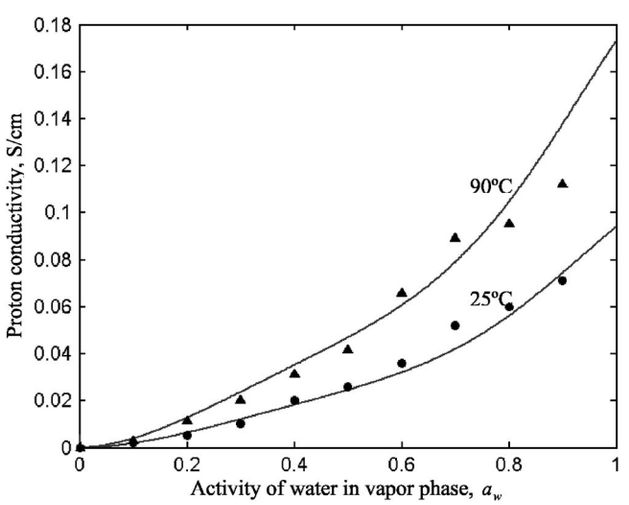


**Figure 6.** Proton conductivity of Nafion/($ZrO_2/SO_4^{2-}$) at 25 and 90°C.

*Worcester Polytechnic Institute assisted in meeting the publication costs of this article.*

## References

1. G. Alberti and M. Casciola, *Annu. Rev. Mater. Res.*, **33**, 129 (2003).
2. B. C. H. Steele and A. Heinzel, *Nature (London)*, **414**, 345 (2001).
3. P. Jannasch, *Curr. Top. Colloid Interface Sci.* **8**, 96 (2003).
4. Q. Li, R. He, J. O. Jensen, and N. J. Bjerrum, *Chem. Mater.*, **15**, 4896 (2003).
5. C. Yang, P. Costamagna, S. Srinivasan, J. Benziger, and A. B. Bocarsly, *J. Power Sources*, **103**, 1 (2001).
6. N. Miyake, J. S. Wainright, and R. F. Savinell, *J. Electrochem. Soc.*, **148**, A905 (2001).
7. A. S. Arico, V. Baglio, A. Di Blasi, and V. Antonucci, *Electrochem. Commun.*, **5**, 862 (2003).
8. A. S. Arico, V. Baglio, A. Di Blasi, P. Creti, P. L. Antonucci, and V. Antonucci, *Solid State Ionics*, **161**, 251 (2003).
9. H. Uchida, Y. Ueno, H. Hagihara, and M. Watanabe, *J. Electrochem. Soc.*, **150**, A57 (2003).
10. T. M. Thampan, N. H. Jalani, P. Choi, and R. Datta, *J. Electrochem. Soc.*, **152**, A316 (2003).
11. P. Costamagna, C. Yang, A. B. Bocarsly, and S. Srinivasan, *Electrochim. Acta*, **47**, 1023 (2002).
12. S. Malhotra and R. Datta, *J. Electrochem. Soc.*, **144**, L23 (1997).
13. V. Ramani, H. R. Kunz, and J. M. Fenton, *J. Membr. Sci.*, **232**, 31 (2004).
14. S. P. Nunes, B. Ruffmann, E. Rikowski, S. Vetter, and K. Richau, *J. Membr. Sci.*, **203**, 215 (2002).
15. B. Bonnet, D. J. Jones, J. Roziere, L. Tchicaya, G. Alberti, M. Casciola, L. Massinelli, B. Bauer, A. Peraio, and E. Ramunni, *J. New Mater. Electrochem. Syst.*, **3**, 87 (2000).
16. M. L. Ponce, L. Prado, B. Ruffmann, K. Richau, R. Mohr, and S. P. Nunes, *J. Membr. Sci.*, **217**, 5 (2003).
17. P. Staiti, *Mater. Lett.*, **47**, 241 (2001).
18. W. Apichatachutapan, R. B. Moore, and K. A. Mauritz, *J. Appl. Polym. Sci.*, **62**, 417 (1996).
19. Q. Deng, R. B. Moore, and K. A. Mauritz, *J. Appl. Polym. Sci.*, **68**, 747 (1998).
20. P. Liu, J. Bandara, Y. Lin, D. Elgin, L. F. Allard, and Y. P. Sun, *Langmuir*, **18**, 10389 (2002).
21. K. T. Adjemian, S. J. Lee, S. Srinivasan, J. Benziger, and A. B. Bocarsly, *J. Electrochem. Soc.*, **149**, A256 (2002).
22. P. Choi, N. H. Jalani, and R. Datta, *J. Electrochem. Soc.*, **152**, E84 (2005).
23. P. Choi, N. H. Jalani, and R. Datta, *J. Electrochem. Soc.*, **152**, E123 (2005).
24. P. W. Atkins, *Physical Chemistry*, 3rd ed., W.H. Freeman and Company, New York (1986).
25. S. Mafe, J. A. Manzanares, and P. Ramirez, *Phys. Chem. Chem. Phys.*, **5**, 376 (2003).
26. D. Marx, M. E. Tuckerman, J. Hutter, and M. Parrinello, *Nature (London)*, **397**, 601 (1999).
27. M. E. Tuckerman, *J. Phys.: Condens. Matter*, **14**, R1297 (2002).
28. M. E. Tuckerman, D. Marx, and M. Parrinello, *Nature (London)*, **417**, 925 (2002).

29. N. Agmon, *J. Phys. Chem.*, **100**, 1072 (1996).
30. S. Meiboom, *J. Chem. Phys.*, **34**, 375 (1961).
31. J. O'M. Bockris and A. K. N. Reddy, *Modern Electrochemistry*, Vol. 1, Plenum Press, New York (1998).
32. T. Thampan, S. Malhotra, H. Tang, and R. Datta, *J. Electrochem. Soc.*, **147**, 3242 (2000).
33. C. Ma, L. Zhang, S. Mukerjee, D. Ofer, and B. Nair, *J. Membr. Sci.*, **219**, 123 (2003).
34. K. D. Kreuer, *J. Membr. Sci.*, **185**, 29 (2001).
35. E. Glueckauf and G. P. Kitt, *Proc. R. Soc. London, Ser. A*, **228**, 322 (1955).
36. G. A. Olah, G. K. S. Prakash, and J. Sommer, *Superacid*, John Wiley & Sons, New York (1985).
37. R. S. Drago and N. Kob, *J. Phys. Chem. B*, **101**, 3360 (1997).
38. F. Haase and J. Sauer, *J. Am. Chem. Soc.*, **120**, 13503 (1998).
39. S. Koter, *J. Membr. Sci.*, **206**, 201 (2002).
40. B. Li and R. D. Gonzalez, *Ind. Eng. Chem. Res.*, **35**, 3141 (1996).
41. T. Kanougi, T. Atoguchi, and S. Yao, *J. Mol. Catal. A: Chem.*, **177**, 289 (2002).
42. A. R. Ramadan, N. Yacoub, and J. Ragai, *J. Mater. Sci.*, **39**, 1383 (2004).
43. K. Arata and M. Hino, *Mater. Chem. Phys.*, **26**, 213 (1990).
44. M. T. Tran, N. S. Gnep, G. Szabo, and M. Guisnet, *Appl. Catal., A*, **171**, 207 (1998).
45. M. Eikerling, A. A. Kornshev, A. M. Kuznetsov, J. Ulstrup, and S. Walbran, *J. Phys. Chem. B*, **105**, 3646 (2001).
46. P. Commer, A. G. Cherstvy, E. Spohr, and A. A. Kornshev, *Fuel Cells*, **2**, 127 (2002).
47. J. Ennari, M. Elomaa, and F. Sundholm, *Polymer*, **40**, 5035 (1999).
48. B. Cohen and D. Huppert, *J. Phys. Chem. B*, **107**, 3598 (2003).
49. N. Agmon, *Chem. Phys. Lett.*, **244**, 456 (1995).
50. J. H. Simpson and H. Y. Carr, *Phys. Rev.*, **111**, 1201 (1958).
51. P. Berezanski, in *Handbook of Instrumental Techniques for Analytical Chemistry*, Chap. 39, pp. 749-764, F. Settle, Editor, Prentice-Hall, Upper Saddle River, NJ (1997).
52. B. D. Cornish and R. J. Speedy, *J. Phys. Chem.*, **88**, 1888 (1984).
53. N. H. Jalani, K. Dunn, and R. Datta, *Electrochim. Acta*, In press.